TECHNICAL
RESEARCH
REPORT

SYSTEMS
RESEARCH
CENTER

*Supported by the
National Science Foundation
Engineering Research Center
Program (NSFD CD 8803012),
Industry and the University*

Computer Assisted Tomography Applied to Plasma Electron Distribution Functions

*by S. Li, Q. Lin, M.A. Coplan,
J.H. Moore, and C.A. Berenstein*

TR 92-38

Computer Assisted Tomography

Applied to Plasma Electron Distribution Functions

S. Li*, Q. Lin*, M.A. Coplan*,

J.H. Moore+,

C.A. Berenstein**

Abstract

We consider several possible instruments based on Computer Tomography to determine space plasma distribution functions.

* Partially supported by NASA grants NAG-5-1129/924/1149

** Partially supported by NSF grants CDR-8803012 and DMS-9000619

COMPUTER ASSISTED TOMOGRAPHY APPLIED TO PLASMA ELECTRON DISTRIBUTION FUNCTIONS

Shixiong Li* and Qipeng Lin**
Department of Mathematics, Anhui University
Anhui 230039, P. R. of China

M. A. Coplan
Institute for Physical Science and Technology, University of Maryland
College Park, Maryland 20742

J. H. Moore
Department of Chemistry and Biochemistry, University of Maryland
College Park, Maryland 20742

C. A. Berenstein
Department of Mathematics, University of Maryland
College Park, Maryland 20742

I. Introduction

An instrument that measures the line integrals of the electron velocity distribution function of a space plasma is an attractive alternative to the conventional method of measuring individual points on the distribution function itself. Y. Zhang, M. Coplan, J.H. Moore and C.A. Berenstein in their paper "Computerized tomographic imaging for space plasma physics" explained the fundamental principles and suggested a simple two-dimension magnetic field model instrument. They also point out that there are a variety of electric and magnetic field configurations upon which the design of a tomographic plasma probe can be based. In this report, we consider a number of different configurations upon which instruments for line-integral measurements of electron velocity

* Visiting Scholar, Institute for Physical Science and Technology
University of Maryland, College Park, Maryland 20742

** Visiting Scholar, Institute for Physical Science and Technology
University of Maryland, College Park, Maryland 20742

distribution functions could be based along with the mathematical principles and algorithms to reconstruct image functions from the line integrals.

II. Instrument Configurations for Line-Integral Measurements of Electron Velocity Distribution Functions

A. Consider a box B inside of which a constant electrostatic field **E** is present. Assume the field has intensity E and the direction of E is parallel to the x-axis (Fig. 1).

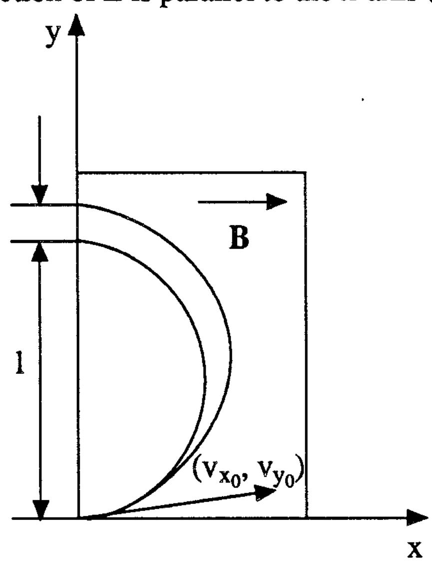

Figure 1

The motion of an electron entering the box through the aperture O is describe by the equations

$$x(t) = -\frac{\alpha t^2}{2} + v_{x_0} t$$

$$y(t) = v_{y_0} t \qquad \text{(II 1)}$$

where $\alpha = eE / m$, m is the electron mass, -e the electron charge, (v_{x_0}, v_{y_0}) the velocity of an electron entering the aperture. Now assume that the side of the box at x = 0 is a detector consisting of independent collectors that count the number of electrons that impinge upon them. If an electron hits a collector with coordinate $(0,\ell)$ at time t_o, from equations (II 1) we obtain

$$0 = -\frac{\alpha t^2}{2} + v_{x_o} t_o$$

$$\ell = v_{y_o} t_o \qquad \text{(II 2)}$$

From (II 2), we obtain

$$v_{x_o} = \frac{\alpha t_o}{2}, \; t_o = \frac{\ell}{v_{y_o}}$$

Finally we get

$$v_{x_o} v_{y_o} = \frac{\alpha \ell}{2} \qquad \text{(II 3)}$$

In (v_{xo}, v_{yo}) space, the equation (II 3) is a hyperbola. Using this idea, we can obtain the line integrals of the electron velocity distribution function along families of hyperbolas. Suppose the width of the pixel is $\Delta\ell$, the velocity (v_{x_o}, v_{y_o}) of the electrons that impinge upon the collector must lie within the strip S (Figure 2).

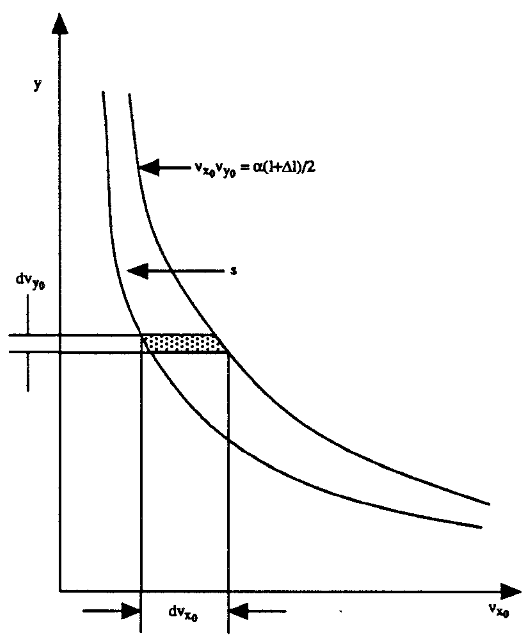

Figure 2

The width of the strip S is $\Delta v_{x_o} = \dfrac{\alpha\Delta\ell}{2v_{y_o}}$ (II 4)

The number of electrons counted per second by the collector located at $(0,\ell)$ with width $\Delta\ell$ is

$$\frac{dN}{dt} = An_e\int_0^\infty f(v_x,v_y)v_x\Delta v_x dv_y$$

$$= An_e\int_0^\infty f(\frac{\alpha\ell}{2v_y},v_y)\frac{\alpha\ell}{2v_y}\frac{\alpha\Delta\ell}{2v_y}dv_y \quad \text{(II5)}$$

$$= \frac{An_e\alpha^2\ell\Delta\ell}{4}\int_0^\infty f(\frac{\alpha\ell}{2v_y},v_y)\frac{dv_y}{v_y} \quad \text{(II6)}$$

where n_e is the electron density, and A is the area of the entrance aperture. Let ds be the differential of the arc length of the hyperbola (II 3), we have

$$ds = \sqrt{dv_x^2+dv_y^2} = \sqrt{1+\left(\frac{dv_x}{dv_y}\right)^2}\,dv_y = \frac{\sqrt{v_x^2+v_y^2}}{v_y}dv_y \quad \text{(II 7)}$$

So we may rewrite eq. (II 7) in the following form

$$\frac{dN}{dt} = \frac{An_e\alpha^2\ell\Delta\ell}{4}\int_{C_{\frac{\alpha\ell}{2}}} f(v_x,v_y)\frac{2v_x}{\alpha\ell\sqrt{v_x^2+v_y^2}}ds$$

$$= \frac{An_e\alpha\Delta\ell}{2}\int_{C_{\frac{\alpha\ell}{2}}} f(v_x,v_y)\frac{v_x}{\sqrt{v_x^2+v_y^2}}ds \quad \text{(II 8)}$$

Where $\int_{C_{\frac{\alpha\ell}{2}}}$ denotes the line integral along the hyperbola $v_xv_y = \frac{\alpha\ell}{2}$ (v_x, $v_y > O$). Therefore, $\frac{dN}{dt}$ is the generalized Radon transform of the function $f(v_x,v_y)\frac{v_x}{\sqrt{v_x^2+v_y^2}}$ along the hyperbola $v_xv_y = \frac{\alpha\ell}{2}$. If we rotate the instrument by an angle θ, in the new coordinate system (x', y') (Figure 3), we have

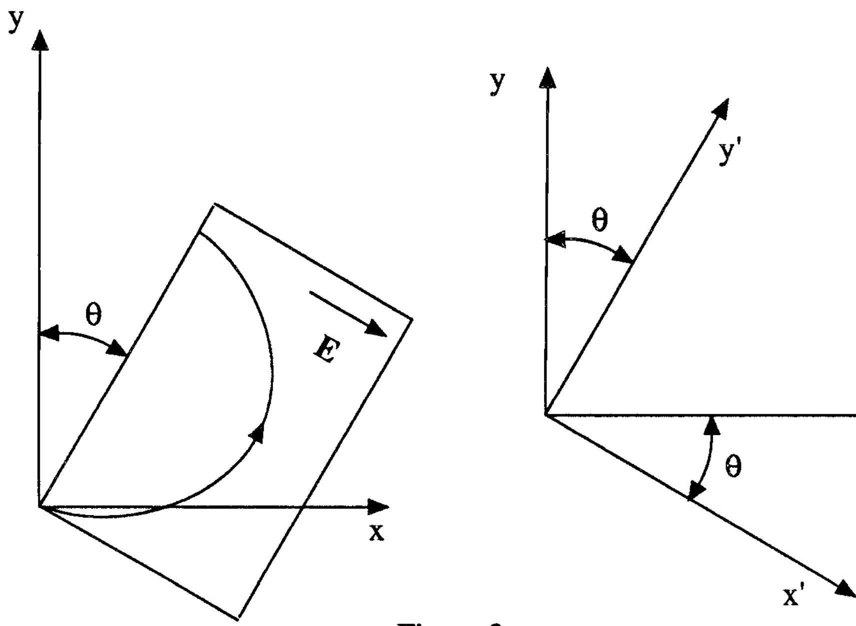

Figure 3

$$
\begin{aligned}
v_x' &= v_x\cos\theta - v_y\sin\theta \\
v_y' &= v_x\sin\theta + v_y\cos\theta
\end{aligned}
\qquad \text{(II9)}
$$

$$
\begin{aligned}
v_x'v_y' &= (v_x\cos\theta - v_y\sin\theta)(v_x\sin\theta + v_y\cos\theta) \\
&= (v_x^2 - v_y^2)\frac{\sin 2\theta}{2} + v_x v_y \cos 2\theta \\
&= \frac{1}{2}(v_x^2 - v_y^2)\cos\phi + v_x v_y \sin\phi
\end{aligned}
\qquad \text{(II10)}
$$

The hyperbola $v_x'v_y' = \frac{\alpha\ell}{2}$ in the (x',y') coordinate system corresponds to the hyperbola $(v_x^2 - v_y^2)\cos\phi + 2v_xv_y\sin\phi =$ in the (x,y) coordinate system (denoted by $C_{\alpha\ell,\phi}$). For different ℓ and ϕ, we get families of curves that will be considered in more detail in II A. We can reconstruct the velocity distribution source function by the method of conformal mapping suggested in IIIA. There still remains one problem; the output of the collector is the Radon transform of the function, $f(v_x,v_y)\frac{v_x}{\sqrt{v_x^2+v_y^2}}$ when we rotate the instrument through an angle θ. The factor $\sqrt{v_x^2+v_y^2}$ in the denominator does not present any difficulties, because $v_x^2 + v_y^2$ is invariant under the rotation of the coordinate system:

$$v_x^2 + v_y^2 = v'_x{}^2 + v'_y{}^2 \qquad \text{(II 11)}$$

On the other hand, the factor v_x in the numerator can cause difficulties. From eq. (II 9), as we rotate the instrument through the angle θ, we obtain the generalized Radon transform of along the hyperbola $C_{\alpha\ell,\phi}$ (denoted by Rf 1). So that, for an angle θ, we get the Radon transform of different functions. We cannot reconstruct the velocity distribution function from such data. We can overcome this problem by using a second box B_2 (Figure 4) is perpendicular to the first box (denoted by B_1).

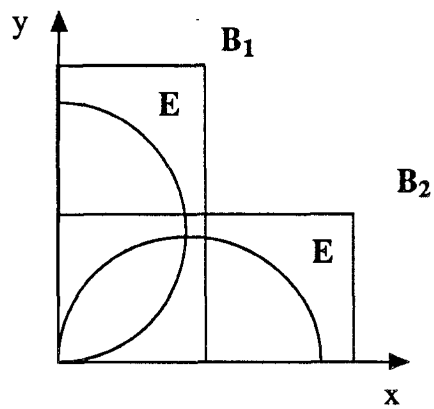

Figure 4

The collectors of the second box, give the generalized radon transform of the function along hyperbola $v_x v_y = \frac{\alpha\ell}{2}$. When we rotate the box B_2 through an angle θ, we get the generalized Radon transform of $f(v_x, v_y)\frac{v_x \sin\theta + v_y \cos\theta}{\sqrt{v_x^2 + v_y^2}}$ along hyperbola $C_{\alpha l,\phi}$ (denoted by Rf 2).

Obviously, we have

$$\cos\theta Rf1 + \sin\theta Rf2 = \int_{C_{\alpha\ell,\phi}} f(v_x, v_y)\frac{v_x}{\sqrt{v_x^2 + v_y^2}} ds \qquad \text{(II12)}$$

These are not the data we need to reconstruct the velocity distribution source function.

B . Consider a more general case. The constant electrostatic field presented has an arbitrary direction ϕ, and the collector D is placed at (ξ,η).

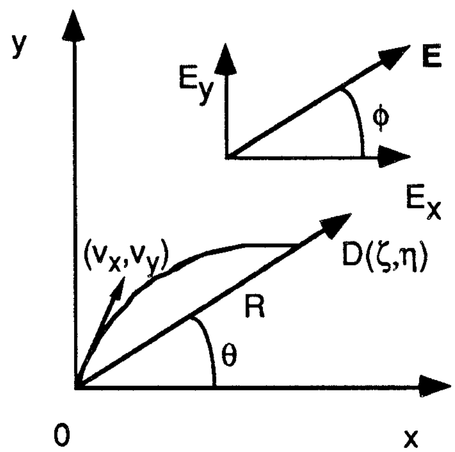

Figure 5

Let $\alpha_1 = \frac{eE_x}{m}$, $\alpha_2 = \frac{eE_y}{m}$, $\alpha = \frac{eE}{m}$, $\xi = R\cos\theta$, $\eta = R\sin\theta$

then

$$E_x = E\cos\phi,\ E_y = E\sin\phi,\ \alpha_1 = \alpha\cos\phi,\ \alpha_2 = \sin\phi$$

Now the motion of electron is described by the equations

$$x(t) = -\frac{\alpha_1 t^2}{2} + v_x t$$

$$y(t) = -\frac{\alpha_2 t^2}{2} + v_y t \qquad \text{(II13)}$$

If an electron hits the collector with coordinate (ξ,η) at time t_o, by eq (II 13), we have

$$\xi = -\frac{\alpha_1 t^2}{2} + v_x t_0$$

$$\eta = -\frac{\alpha_2 t^2}{2} + v_y t_0 \qquad \text{(II 14)}$$

eliminating t_o from (II 14), we obtain

$$\alpha_2 \eta v_x^2 + \alpha_1 \xi v_y^2 - (\alpha_2 \xi + \alpha_1 \eta) v_x v_y + \frac{1}{2}(\alpha_2 \xi - \alpha_1 \eta)^2 = 0 \qquad \text{(II 15)}$$

or

$$\sin\phi\sin\theta v_x^2+\cos\phi\cos\theta v_y^2-(\sin\phi\cos\theta+\cos\phi\sin\theta)v_xv_y+\frac{R\alpha}{2}(\sin\phi\cos\theta-\cos\phi\sin\theta)^2=0 \tag{II 16}$$

If we take the special case $\phi=\frac{\pi}{2}+\theta$, then (II 16) reduces to

$$(vx^2 - vy^2)\sin 2\theta + 2v_xv_y\cos 2\theta = R\alpha$$

The special case we have considered in IIA. If we take the case $\theta=\frac{\pi}{2}$, then (II 16) reduces to

$$v_x^2\sin\phi - v_xv_y\cos\phi+\frac{R\alpha}{2}\cos^2\phi=0 \tag{II 17}$$

This is also a family of hyperbolas, but non-equilateral hyperbolae. The conformal mapping method suggested in IIB fails for this case. Although we can use "Algebraic Reconstruction Technique" (ART) to recover the image function, it requires a great deal of computing time, and gives a poor image. The establishing of a simple and accurate algorithm to reconstruct the image function from this kind of generalized Radon transform (G.R.T.) is an interesting and valuable mathematical problem.

C. Magnetic Field in Three Dimensional Case

Consider a box C, inside of which there is a constant magnetic field. The field has intensity **B** in the Z-direction. The motion of an electron entering box C through the aperture O is described by the equations

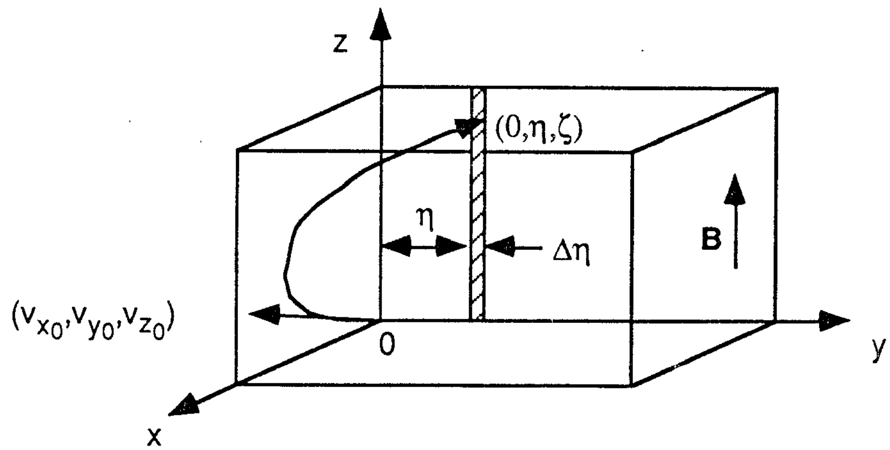

Figure 6

$$m\frac{d^2x}{dt^2} = \left(\frac{e}{c}\right)Bv_y$$
$$m\frac{d^2y}{dt^2} = \left(\frac{e}{c}\right)Bv_x$$
$$m\frac{d^2z}{dt^2} = 0 \qquad \text{(II18)}$$

where M, e, (v_x, v_y, v_z) are the mass, charge and velocity of the electron respectively, and c is the speed of light. Solving these equations, we obtain

$$x(t) = \frac{1}{\gamma}\left[v_{x_o}\sin\gamma t - v_{y_o}\cos\gamma t\right] + x_o$$
$$y(t) = \frac{1}{\gamma}\left[v_{x_o}\cos\gamma t + v_{y_o}\sin\gamma t\right] + y_o$$
$$z(t) = v_{z_o}t \qquad \text{(II19)}$$

where $\gamma = eB/mc$, $(v_{x_0}, v_{y_0}, v_{z_0})$ are the velocity components of the electron at the aperture, and $x_o = \frac{1}{\gamma}v_{y_o}, y_o = -\frac{1}{\gamma}v_{x_o}$. Now assume an electron hits a collector with coordinates (0,η,ξ) at time t_o, we have

$$0 = \frac{1}{\gamma}\left[v_{x_o}\sin\gamma t - v_{y_o}\cos\gamma t\right] + x_o$$
$$\eta = \frac{1}{\gamma}\left[v_{x_o}\cos\gamma t + v_{y_o}\sin\gamma t\right] + y_o$$
$$\zeta = v_{z_o}t \qquad \text{(II20)}$$

Eliminating t_o from the above equations, we obtain

$$v_{x_o} = -\frac{\gamma\eta}{2}$$
$$v_{y_o} = \frac{\gamma\eta}{2}\cot\left(\frac{\gamma\zeta}{2v_{z_o}}\right) \qquad \text{(II21)}$$

Let η be fixed, ζ varies from $-\infty$ to ∞, (that means the collector is a long strip). It is easy to verify that the velocity of the electrons which impinge upon the collector, constitute the plane $v_{x_o} = -\frac{\gamma\eta}{2}$ in the velocity space. If the collector has a width $\Delta\eta$, then the number of electrons counted by the collector per unit time is

$$\frac{dN}{dt} = An_e v_x \Delta v_x \int\int_{-\infty}^{\infty} f(v_x, v_y, v_z) dv_y dv_z \qquad \text{(II22)}$$

where $f(v_x,v_y,v_z)$ is the electron velocity distribution function, n_e is the electron density, and A is the area of the entrance aperture. By rotating the box in space, the three dimensional Radon transform of $f(v_x,v_y,v_z)$ is obtained. By the method suggested of IIC we can therefore reconstruct the velocity distribution function $f(v_x,v_y,v_z)$ from the recorded data.

D. Combination of Electro-static and Magnetic Fields

Consider the general case where electric and magnetic fields are presented simultaneously. The motion of an electron entering box C through the aperture O is described by the equations

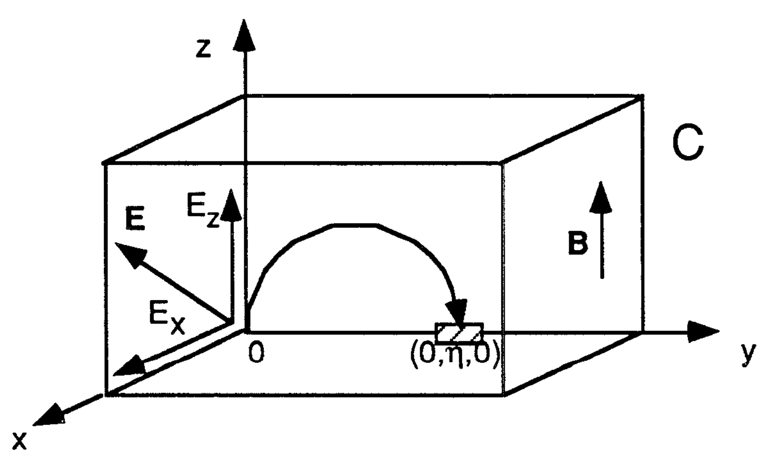

Figure 7

$$m\frac{d^2x}{dt^2} = \left(\frac{e}{c}\right)Bv_y - E_1e$$
$$m\frac{d^2y}{dt^2} = -\left(\frac{e}{c}\right)Bv_x$$
$$m\frac{d^2z}{dt^2} = -E_2e \qquad \text{(II 23)}$$

Let $\gamma = \frac{eB}{mc}$, $\alpha_1 = \frac{eE_1}{m}$, $\alpha_2 = \frac{eE_2}{m}$, then solving these equations, we obtain,

$$x(t) = \frac{1}{\gamma}\left[v_{x_o}\sin\gamma t - (v_{y_o} - \frac{\alpha_1}{\gamma})\cos\gamma t\right] + x_o$$
$$y(t) = \frac{1}{\gamma}\left[v_{x_o}\cos\gamma t + (v_{y_o} - \frac{\alpha_1}{\gamma})\sin\gamma t\right] + y_o + \frac{\alpha_1}{\gamma}t$$
$$z(t) = v_{z_o}t - \frac{\alpha_2 t^2}{2} \qquad \text{(II 24)}$$

where (v_{xo}, v_{yo}, v_{zo}) is the velocity of the electron at the aperture, and

$x_o = \frac{1}{\gamma}(v_{y_o} - \frac{\alpha_1}{\gamma})$, $y_o = -\frac{1}{\gamma}v_{x_o}$, $t_o = \frac{2v_{z_o}}{\alpha_2}$. Then for the electron striking the collector at $(0,\eta,0)$,

$$-\frac{1}{\gamma}(v_{y_o} - \frac{\alpha_1}{\gamma}) = \frac{1}{\gamma}\left[v_{x_o}\sin\gamma t_o - (v_{y_o} - \frac{\alpha_1}{\gamma})\cos\gamma t_o\right]$$
$$\eta + \frac{v_{x_o}}{\gamma} - \frac{2\alpha_1 v_{z_o}}{\gamma\alpha_2} = \frac{1}{\gamma}\left[v_{x_o}\cos\gamma t_o + (v_{y_o} - \frac{\alpha_1}{\gamma})\sin\gamma t_o\right] \qquad \text{(II 25)}$$

Eliminating t_o from the above equations, we obtain

$$(v_{y_o} - \frac{\alpha_1}{\gamma})^2 + (\gamma\eta + v_{x_o} - \frac{2\alpha_1 v_{z_o}}{\alpha_2})^2 = v_{x_o}{}^2 + (v_{y_o} - \frac{\alpha_1}{\gamma})^2$$

simplifying, we obtain

$$\frac{4\alpha_1{}^2}{\alpha_2{}^2}v_{z_o}{}^2 - \frac{4\alpha_1}{\alpha_2}v_{z_o}v_{x_o} - \frac{4\alpha_1\gamma\eta}{\alpha_2}v_{z_o} + 2\gamma\eta v_{x_o} + \gamma^2\eta^2 = 0 \qquad \text{(II 26)}$$

This is also family of hyperbolae which depends upon the three parameters α_1, α_2 and γ. This suggests the possibility of different line-integral measurement instruments, but there is also the issue of inverting the G.R.T. as discussed in IIB.

III. INVERSION OF THE RADON TRANSFORM—MATHEMATICAL FOUNDATIONS AND COMPUTER IMPLEMENTATION

A. The Method of Filtered Back projection.

The filtered back projection reconstruction algorithm is the most important algorithm for inversion of the classical Radon transform. The key to the implementation of the selection of this method is a suitable filter function. Let f(x, y), (x, y) $\in R^2$ — Euclidean plane, and g(θ, t), (θ, t) $\in [0, 2\pi; -\infty, \infty]$ are functions of Schwartz class, i.e. rapidly decreasing smooth functions. $\tilde{f}$, $\tilde{g}$ denote the Fourier transforms of f and g:

$$\tilde{f}(\omega_1, \omega_2) = \frac{1}{2\pi}\int\int f(x,y)e^{-i(x\omega_1 + y\omega_2)}dxdy$$
$$\tilde{g}(\theta, \omega) = \frac{1}{2\pi}\int g(\theta, t)e^{-i\omega t}dt \qquad \text{(III 1)}$$

The Radon transform is R: f(x, y) --> R f(q, t) = $\int_{-\infty}^{\infty} f(t\cos\theta - s\sin\theta, t\sin\theta + s\cos\theta)ds$.

The back projection operator $R^{\#}$ is defined by

$$R^{\#}: g(\theta, t) \dashrightarrow R^{\#} g(x, y) = = \int_0^{2\pi} g(\theta, x\cos\theta + y\sin\theta)d\theta. \qquad \text{(III 2)}$$

(We call $R^{\#}$ back projection because it integrates all lines $\ell_{\theta,t} = x\cos\theta + y\sin\theta = t$, passing through point (x, y). The convolution of two functions f_1, f_2 or g_1, g_2 is defined by

$$f_1 * f_2(x,y) = \int_{-\infty}^{\infty}\int_{-\infty}^{\infty} f_1(x-u, y-v) f_2(u,v)\,du\,dv$$

$$g_1 * g_2(\theta,t) = \int g_1(\theta, t-s) g_2(\theta,s)\,ds \qquad \text{(III 3)}$$

It is easy to verify the following relation between the Radon transform, back projection and convolution operations

$$(R^{\#} g) * f(x, y) = R^{\#} (g * R f)(x, y) \qquad \text{(III 4)}$$

Assume f(x, y) is b band limited: $\left|\tilde{f}(\omega_1, \omega_2) = 0\right|, \sqrt{\omega_1^2 + \omega_2^2} \geq 1$ or essential b band limited

$\int\limits_{\sqrt{\omega_1^2+\omega_2^2}\geq b}\int \left|\tilde{f}(\omega_1, \omega_2)\right| d\omega_1 d\omega_2 \leq \varepsilon$. Let $h_b(\theta,t)$ be a suitable filter function that depends on b, so that

$$H_b(x, y) = R^{\#} h_b(x, Y) \qquad \text{(III 5)}$$

Then, by relation (III 4), we have

$$H_b * f(x, y) = (R^{\#} h_b) * f(x, y) = R^{\#} (h_b * R f)(x, y) \qquad \text{(III 6)}$$

If $H_b(x, y) \approx \delta(x, y)$ (Dirac δ function), then we have the inversion formula

$$f(x, y) = \delta * f(x, y) \approx H_b * f(x, y) = R^{\#} (h_b * R f)(x, y) \qquad \text{(III 7)}$$

So the problem becomes the representation of h_b by H_b. It can be proved that, if H_b is a radial function, we have

$$\tilde{h}_b(\theta, \omega) = \tilde{h}_b(\omega) = \frac{1}{4\pi\sqrt{2\pi}} |\omega| \tilde{H}_b(\omega). \qquad \text{(III 8)}$$

It is more convenient to select H_b than h_b, because, by (III 7), we see that the inversion formula is controlled by H_b directly.

Let $\phi(t)$ satisfy : $0 \le \tilde{\phi}(\omega) \le 1,\ \tilde{\phi}(0) = 1, \left|\tilde{\phi}(\omega)\right| = 0,\ |\omega| > 1.$ We may set

$$\tilde{H}_b(\omega) = \tilde{H}_b\left(\sqrt{\omega_1^2 + \omega_2^2}\right) = \tilde{\phi}(\frac{\omega}{b})$$

For example, take

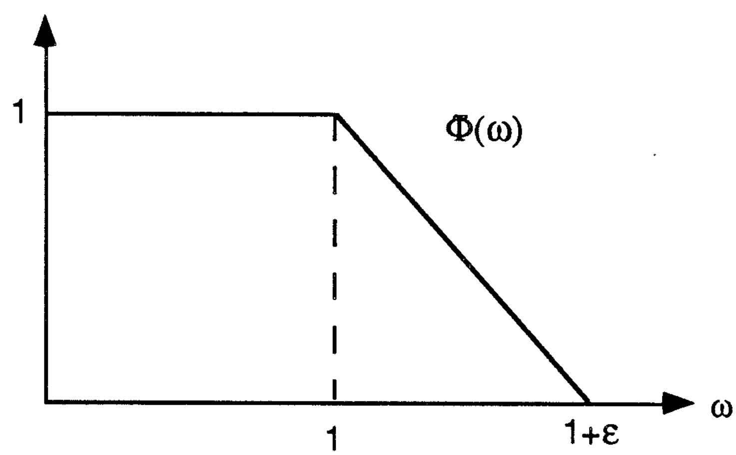

Figure 8

$$\tilde{\Phi}_\varepsilon(\omega) = \begin{cases} 1, & 0 \le \omega \le 1 \\ \left(1 + \frac{1}{\varepsilon}\right) - \frac{\omega}{\varepsilon}, & 1 \le \omega \le 1 + \varepsilon \\ 0, & \omega > 1 + \varepsilon \end{cases}$$

$$\tilde{\Phi}_\varepsilon(-\omega) = \tilde{\Phi}_\varepsilon(\omega) \qquad \text{(III 9)}$$

Then

$$h_{b\varepsilon}(s) = \frac{1}{\sqrt{2\pi}} \int_{-\infty}^{\infty} \tilde{h}_{b\varepsilon}(\omega) e^{i\omega s} d\omega$$

$$= \frac{1}{8\pi^2} \int_{-b(1+\varepsilon)}^{b(1+\varepsilon)} |\omega| \tilde{\Phi}_\varepsilon\left(\frac{|\omega|}{b}\right) e^{i\omega s} d\omega$$

$= [b/4\pi^2 S - (1+\varepsilon)b/4\pi^2 \varepsilon S + b/4\pi^2 \varepsilon S - 2/4\pi^2 \varepsilon S^3 b] \sin(bS)$

$+ [1/4\pi^2 S - (1+\varepsilon)/4\pi^2 \varepsilon S - 2/4\pi^2 \varepsilon S^2]$

$+ [2/4\pi^2 \varepsilon S^3 b] \sin(1+\varepsilon)bS$

$+ [-(1+\varepsilon)/4\pi^2 \varepsilon S^2] \cos(1+\varepsilon)bS - 1/4\pi^2 S^2, \quad S \neq 0$

$h_{b\varepsilon}(0) = b^2/24\pi^2(3 + 3\varepsilon + \varepsilon^2)$ (III 10)

for the special case $\varepsilon = 1$, we have

$n_{b1}(0) = 7b^2/24\pi^2$,

$h_{b1}(S) = 1/4\pi^2[-2/S^3 b \sin bS + 1/S^2 \cos bS + 2/S^3 b \sin^2 bS - 2/S^2 \cos bS - 1/S^2]$ (III 11)

To implement this numerically we need a discrete version of the filter back projection method. Suppose $f(x, y)$ is supported within $x^2 + y^2 \leq R^2$ and is essentially b band limited, then its Radon transform $Rf(\theta, t)$ is also supported within $x^2 + y^2 \leq R^2$. If $Rf(\theta, t)$ is sampled at

$\theta j = 2\pi/p(j - 1), j = 1, 2, ..., p$ (III 12)

$t_k = R/l\ (k), \qquad k = 0, \pm 1, \pm 2, ..., \pm l$

According to the Shannon Sampling Theorem here $R/l = h$, $h = \pi/2b$, and $p = [\pi l]$. (Because the filter function is 2b band limited)

$$h_{b1}(t_k) = \begin{cases} 7b^2/24\pi^2, & k = 0 \\ b^2/\pi^4 k^2 - 4b^2/\pi^5 k^5, & k = 4n = 1 \\ -4b^2/\pi^4 k^2, & k = 4n + 2 \\ 4b^2/\pi^5 k^3 + b^2/\pi^4 k^2, & k = 4n + 3 \\ -2b^2/\pi^4 k^2, & k = 4n \end{cases}$$

Now the discrete filter operator takes the form:

$$v_{j,k} = \frac{R}{l} \sum_{S=-l}^{l} h_{b1}(t_k - t_s) Rf(\theta_j, t_s) \qquad \theta j = 2\pi/p(j - 1),\ j = 1, 2, ..., p$$

$$t_k = R/l\ (k), \qquad k = 0, \pm 1, \pm 2, ..., \pm l \qquad \text{(III 14)}$$

and the discrete back projection takes the form:

$$f(x,y) = \frac{2\pi}{p} \sum_{j=1}^{p} \left[(1-u)v_{j,k} + uv_{j,k+1}\right] \qquad \text{(III 15)}$$

here $u = s_j / h - k$, $k \le s_j / h \le k + 1$, $s_j = x \cos \theta_j + y \sin \theta_j$

(III 14) and (III 15) are just the formula we need for numerical computation. For model examples, see IV.

B. Inversion of Generalized Radon Transform — Method of Conformal Mapping.

Given two functions u(x, y), v(x, y) on the Euclidean plane, let $C_{\theta,t}$: $u(x, y) \cos \theta + v(x, y) \sin \theta = t$ denotes the family of curves which depends upon the two parameters θ and t . If f(x, y) is a given function, we call the line integral of f(x, y) along the family of curves $C_{\theta,t}$

$$Rf_C(\theta,t) = \int_{C_{\theta,t}} f(x,y)ds \qquad \text{(III 16)}$$

The Generalized Radon Transform. (G.R.T.)

It is different to invert the G.R.T. for arbitrary u and v. We have suggested a Conformal Mapping method that can be used to invert the G.R.T. when u and v are a pair of conjugate harmonic functions. It is accurate and convenient for numerical computation. For $u = x^2 - y^2$, $v = 2 x y$, it is a pair of conjugate harmonic functions, exactly the case we have considered in II.

Let function z = F(w) map domain D on the w (= u + i v) plane to domain *D* on the z (= x + iy) plane conformally. Under this mapping, the family of straight lines $l_{\theta,t}$ on the w plane: $l_{\theta,t}$: $u \cos \theta + v \sin \theta = t$ maps to the family of curves $L_{\theta,t}$ on the z-plane.

$$L_{\theta,t} : u(x, y) \cos \theta + v(x, y) \sin \theta = t$$

Let the G.R.T. of function f(x, y) along $L_{\theta,t}$ be

$$(Rf)_L(\theta,t) = \int_{L_{\theta,t}} f(x,y)d\sigma \qquad \text{(III 17)}$$

here dσ is the differential of the arc length of $L_{\theta,t}$. Let the differential of arc length of the straight line $l_{\theta,t}$. Then, according to the theory of functions of complex variables, we have

$$d\sigma = \left|\frac{dz}{dw}\right| ds \qquad \text{(III 18)}$$

so that

$$(Rf)_{L(\theta,t)} = \int_{L_{\theta,t}} f(x,y)d\sigma = \int_{l_{\theta,t}} f(F(w))\left|\frac{dz}{dw}\right|ds$$

$$R\left\{f(F(w))\left|\frac{dz}{dw}\right|\right\}_l (\theta,t) \qquad \text{(III 19)}$$

This is the classical Radon transform (along families of straight lines

$l_{\theta,t}$: $u \cos \theta + v \sin \theta = t$) of the function $\bar{f}(u,v) = \bar{f}(w) = f(F(w))\left|\frac{dz}{dw}\right|$. We can reconstruct the function $\bar{f}(u,v)$ by the method of III A, then the inversion of G.R.T. can be obtained easily.

$$f(x,y) = f(z) = \bar{f}(w(z)) / \left|\frac{dz}{dw}\right| \qquad \text{(III 20)}$$

Let us consider some mapping functions $z = F(w)$, G.R.T. along various kinds of curves

Example 1 $z = F(w) = (\pi + i\, w) / (\pi\, i + w)$, or $w = \pi\, (1 - i\, z) / (z - 1)$

so $u = 2\, \pi\, x / (x^2 + (y - 1)^2)$, $v = \pi\, (1 - x^2 - y^2) / (x^2 + (y - 1)^2)$, $|dz / dw| = x^2 + (y - 1)^2 / 2\pi$

$L_{\theta,t}$: $2\, \pi\, x / (x^2 + (y - 1)^2) \cos \theta + \pi\, (1 - x^2 - y^2) / (x^2 + (y - 1)^2) \sin \theta = t$.

These are circles, with centers at $(\pi \cos q / (t + \pi \sin q), t / (t + \pi \sin \theta))$ with radii equal to $\pi / |\pi \sin \theta + 1|$. All these circles pass through the point (0, 1)).

Example 2 $w = z^2$, so $u = x^2 - y^2$, $v = 2\, x\, y$, $\left|\frac{dz}{dw}\right| = \frac{1}{2\sqrt{x^2 + y^2}}$

$L_{\theta,t}$: $(x^2 - y^2) \cos \theta + 2\, x\, y \sin \theta = t$. This is just the case we have considered in II.

C. Inversion of Radon Transform for the Three Dimensional Case (Surface integral of a function along planes)

Let $P(\theta,p)$ be the plane perpendicular to unit vector $\theta = (a, b, c)$ and lying at a (signed) distance p from the origin. $f(x, y, z)$ is a function of three variables, and the Radon transform $Rf(\theta, p)$ is then

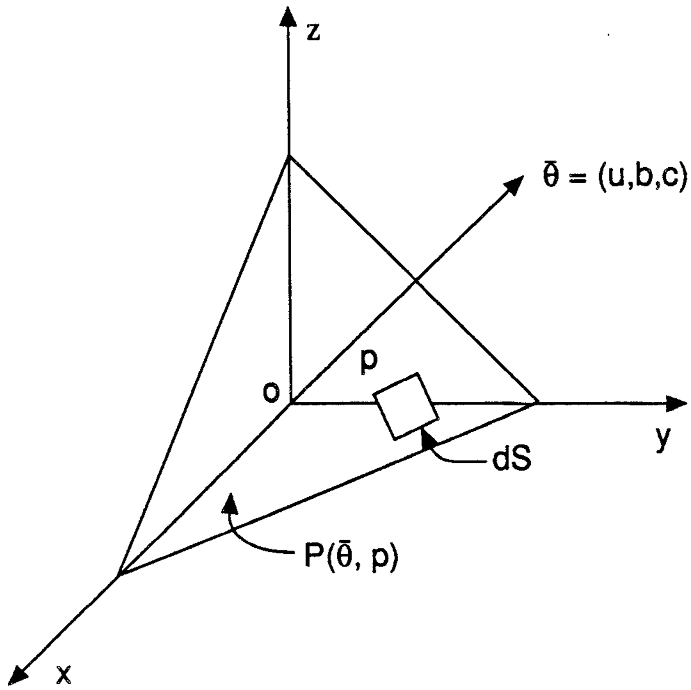

Figure 9

$$Rf(\theta,p) = \iint_{P(\theta,p)} f(x,y,z)dS \qquad \text{(III 21)}$$

here dS is the differential of the surface area of plane $P_{\theta,p}$, θ is unit vector $a^2 + b^2 + c^2 = 1$..

Using the Fourier Slice Theorem.

$$\tilde{f}(w,\theta) = \int_{-\infty}^{+\infty} Rf(\theta,p)e^{-iwp}dp$$

and the Fourier inversion formula, it is easy to derive the following inversion formula for the Radon transform in three dimensions.

$$f(x,y) = \frac{-1}{8\pi^2} \oiint_{S^2} \frac{\partial^2 Rf(\theta,p)}{\partial p^2} d\theta \qquad \text{(III 22)}$$

here S^2 is the unit sphere. To implement the inversion formula (III 22) numerically one must calculate second derivatives $\frac{\partial^2 Rf(\theta,p)}{\partial p^2}$ from the observed $Rf(\theta,p)$ data. Ordinary finite difference methods are unstable with respect to noise but the Spline Fit Method works well.

D. Inversion of the Radon Transform for Linear Combinations of Gaussian Distributions.

Consider the problem of determining the velocity distribution function of electrons in a space plasma, where the function we need to reconstruct is a linear combination of Gaussian functions. For these types of functions, there is a simple method for the reconstruction of the image function.

Let $f(x,y) = Ae^{-\frac{x^2+y^2}{B^2}}$, then $Rf(\theta,p) = A\int_{-\infty}^{+\infty} e^{-\frac{(t\cos\theta - s\sin\theta)^2+(t\sin\theta+s\cos\theta)^2}{B^2}} ds$

$$=f(x,y) = A\int_{-\infty}^{+\infty} e^{-\frac{t^2+s^2}{B^2}} ds = AB\sqrt{\pi}e^{-\frac{t^2}{B^2}} \qquad \text{(III 23)}$$

Now, let $f_i(x, y) = f(x - x_0, y - y_0)$

$$f_i(\theta,t) = \int_{-\infty}^{+\infty} f_i[(t\cos\theta - s\sin\theta) + (t\sin\theta + s\cos\theta)]ds$$

$$= \int_{-\infty}^{+\infty} f(t\cos\theta - s\sin\theta - x_0, t\sin\theta + s\cos\theta - y_0)ds$$

Let $t_0 = t - (x_0 \cos\theta + y_0 \sin\theta)$, $\bar{s} = s + (x_0\sin\theta - y_0\cos\theta)$

We obtain $Rf_i(\theta,t) = \int_{-\infty}^{+\infty} f(t_0\cos\theta - \bar{s}\sin\theta, t_0\sin\theta + \bar{s}\cos\theta)d\bar{s} = Rf(\theta,t_0)$ (III 24)

So, if $\bar{f}(x,y) = Ae^{-\frac{(x-x_0)^2+(y-y_0)^2}{B^2}}$, $Rf(\theta,t) = AB\sqrt{\pi}e^{-\frac{[t-(x_0\cos\theta+y_0\sin\theta)]^2}{B^2}}$ (III25)

for fixed q, $R\bar{f}(\theta,t)$takes the maximum value $AB\sqrt{\pi}$ at $t = x_0 \cos\theta + y_0 \sin\theta$.. The function is a circle in the (t, θ)plane with center at $\left(\frac{x_0}{2},\frac{y_0}{2}\right)$and radius $\frac{\sqrt{x_0^2+y_0^2}}{2}$ It is easy to determine x_0, y_0 and AB directly from the Radon transform of $\bar{f}$.

Let $\theta = tg^{-1}\frac{y_0}{x_0}$, $\sqrt{(x-x_0)^2-(y-y_0)^2} = u$

Then

$$R\bar{f}(\theta,t) = AB\sqrt{\pi}e^{-\frac{u^2}{B^2}}$$

$$x = t\cos\theta, \quad y = t\sin\theta$$

$$u_i = \sqrt{(t_i\cos\theta - x_0)^2 + (t_i\sin\theta - y_0)^2}$$

Let

$$J_0 = AB\sqrt{\pi}, \quad J_i = AB\sqrt{\pi}e^{-\frac{u_i^2}{B^2}}$$

$$\therefore \quad \frac{J_i}{J_0} = e^{-\frac{u_i^2}{B^2}}$$

$$B^2 = \frac{-u_i^2}{\ln\frac{J_i}{J_0}}$$

For practical computation

$$B^2 = \frac{1}{N}\sum_{i=1}^{N}\frac{-u_i^2}{\ln\frac{J_i}{J_0}} \qquad \text{(III 26)}$$

IV. NUMERICAL EXAMPLES

A. Inversion of the classical Radon transform (line integral along families of straight lines) using Method of Filter Back-Projection (F.B.P.) We have used a filter function (III 9) (III 13), which has a gentle cut off to improve the quality of the reconstructed function at the edges.

Fig. IV (1). A three dimensional log plot of the test function representing a velocity distribution function with an anamolous component far in the tail of the main distribution.

$$f(x,y) = \exp(-\frac{x^2+y^2}{2.0}) + \exp(-\frac{(x-4.4)^2+y^2}{12.5})$$

w(x,y) + logf(x,y) + 10.771

z(x,y) = 0.5[w(x,y) + Abs(w(x,y))]

Fig. IV (2). A three dimensional log plot of the image of the function f(x,y) in IV (1), reconstructed from 900 line integrals by method of F.B.P., using the filter function (III 9) (III 13).

Fig. IV (3). A three dimensional log plot of the image of the function f(x,y) in IV (1), reconstructed from 900 line integrals after the introduction of uniform distributed random noise (with standard deviation $0.02/\sqrt{3}$, mathematical expectation 0) on the data, by method of F.B.P., using the filter function (III 9) (III 13).

Fig. IV (4). Two dimensional sections (y = 0) of Fig. IV (1) and Fig. IV (2).

Fig. IV (5). Two dimensional section (y = 0) of Fig. IV (1) and Fig. IV (3).

B. Inversion of Generalized Radon Transform (G.R.T.) (line integrals along family of hyperbolae) by the Method of Conformal Mapping.

Fig. IV (6). A three dimensional plot of the test function

$$f(x,y) = \exp\{-\frac{50}{3}[(x-\sqrt{3}/2)^2 + (y-\sqrt{3}/2)^2]\}$$

Fig. IV (7). A three dimensional plot of the image of the function f(x,y) in IV (6), reconstructed from line integrals of $xf(x,y)/\sqrt{x^2+y^2}$ along families of hyperbolae: $(x^2 - y^2)\cos\theta + 2xy\sin\theta = t$ using the method of conformal mapping.

Fig. IV (8). Same as Fig. IV (7), but after the introduction of uniformly distributed random noise (with mathematical expectation 0 and standard deviation $0.02/\sqrt{3}$) superimposed on the line integral data.

Fig. IV (9). Two dimensional section $(y = \sqrt{3}/2)$ of Fig. IV (6) and Fig. IV (7)

Fig. IV (10). Two dimensional section ($y = \sqrt{3}/2$) of Fig. IV (6) and Fig. IV (8)

C. Inversion of the three dimensional Radon transform (Surface integrals along family of planes)

Fig. IV (11). A two dimensional section ($y = 0, z = 0$) of the test function

$w(x, y, z) = \exp-(x^2 + y^2 + z^2)$